BBAA VI International Colloquium on:
Bluff Bodies Aerodynamics & Applications
Milano, Italy, July, 20–24 2008

VORTEX INDUCED VIBRATIONS AT HIGH REYNOLDS NUMBERS

Giorgio Diana*, Marco Belloli*, Stefano Giappino*, Sara Muggiasca*

*Politecnico di Milano, Dipartimento di Meccanica
Campus Bovisa, Via La Masa 34, 20156 Milano, Italy
e-mails: giorgio.diana@polimi.it, marco.belloli@polimi.it,
stefano.giappino@polimi.it, sara.muggiasca@polimi.it

Keywords: Circular cylinder, Vortex induced vibrations, Reynolds Number, Surface roughness, Wind tunnel tests

Abstract: *Vortex induced vibrations of circular section structures are a well known and deeply studied phenomenon because many engineering applications are involved by this kind of problems. Up to now most part of the experimental results belong to a Reynolds Number range between 500 and* $6 \cdot 10^4$ *and no reliable numerical simulations are available for Reynolds higher than 3000, nevertheless many structures deals with Reynolds of the order of thousands up to more than one million. Vortex shedding studies on still circular cylinder shows that the phenomenon is strongly influenced by the Reynolds Number, in particular in the critical range. In the past Roshko showed that the well defined vortex shedding reappears at postcritical Reynolds Number. Due to the effects of the body surface characteristics on the flow field also the surface roughness affects vortex shedding and it is expected to influence VIV. Because the Reynolds Number is a fundamental parameter in the vortex shedding on fixed cylinder and among all the studies of VIV are at moderate Re, there is the need to understand if and how the Reynolds Number affects also the vortex induced oscillations; in the paper experimental tests on a large diameter cylinder investigate the vortex induced dynamics at high Reynolds Numbers.*

1 INTRODUCTION

Vortex induced vibrations of circular section structures are a well known and deeply studied phenomenon and they can occur in many engineering applications, a general review can be found for instance in [10, 2, 11, 12]. Moreover the large number of contributions by many researchers give evidence of the practical significance of the VIV. Considering an elastically mounted rigid cylinder moving only in cross flow direction, when the frequency of the vortices shed by the cylinder is close enough to the structural frequency of the body, synchronization occurs having the body and the aerodynamic force the same common frequency. In this situation, in particular for light and low damped bodies, large vibration amplitudes occur. It is to note that the lock-in doesn't happen only for wind speeds very close to the Strouhal velocity, but it exists over a wide range of flow velocities. The driven parameters of the fluid-elastic interaction can be attributed to the considered structure (dimensions, mass, damping ratio, natural frequency, surface roughness) and to the fluid (velocity, density, viscosity, turbulence intensity). In spite of this wide set of physical quantities a reduced set of non-dimensional parameters are the key variables that control the free motion response, i.e Scruton Number, mass-ratio and velocity-ratio. Williamson & Roshko in [13] showed that the wake shedding pattern is defined only by the velocity-ratio (or wavelength) and the non-dimensional amplitude. Among these different vortex shedding modes the most important are the 2P and 2S because they exist while the cylinder is experiencing free motion [7, 4], i.e. when the work done by the fluid on the body over a cycle is positive. Up to now most part of the experimental results belong to a Reynolds Number range between 500 and $6 \cdot 10^4$ and no reliable numerical simulations are available for Reynolds higher than 3000 [11]. Vortex shedding studies on still circular cylinder shows that the phenomenon depends on the Reynolds Number and it is well defined in the subcritical Reynolds range while it reduce its magnitude and sometimes disappears in the critical one [16]. In fact, regular vortex shedding can be seriously disrupted if the separation line is not straight [2]. Roshko, in 1961, found that the vortex shedding reappears at higher Reynolds Number in what is now called *post-critical* flow regime when transition occurs within the attached boundary layer and a straight separation line is reestablished [9]. Due to the effects of the body surface characteristics on the boundary layer also the surface roughness affects vortex shedding [5] and it is expected to influence VIV. Because the Reynolds Number is a fundamental parameter in the vortex shedding on fixed cylinder and among all the studies of VIV are at moderate Re, there is the need to understand if and how the Reynolds Number affects also the vortex induced oscillations; in the paper experimental tests on a large diameter cylinder investigate the vortex induced dynamics at high Reynolds Numbers.

2 MODEL AN EXPERIMENTAL SET-UP

Experimental tests were carried out in air at the Politecnico di Milano wind tunnel. The model is a circular section cylinder in carbon fiber having the diameter of $0.72\,m$; it is suspended to the wind tunnel walls by means of tensioned wires realizing a constrain system that allows cross-wind oscillations as visible in Figure 1 and it has two end-plates in order to realize 2D flow conditions. Possible coupling of in-line and torsional motion was avoided through a sufficiently wide separation between the horizontal-vertical and torsional-vertical frequencies. The structural damping is adjusted by adding dampers to the system so that it is possible to vary the Scruton Number. The cylinder has several pressure taps arranged in three different rings connected to high sample-rate pressure scanners that allows the measurement of the aerodynamic force in terms of mean and fluctuating value. The rings are at the distance of 1 diameter

spanwise. Accelerometers are placed on the model to evaluate the displacement in vertical direction. The main mechanical and aerodynamic specifications of the model are summarized in Table 1.

(a) (b)

Figure 1: Cylinder model suspended by cables (a) with added surface roughness (b)

Mechanical characteristics	
Diameter [m]	0.72
Length [m]	3.3
Linear mass [kg/m]	17
Aspect ratio L/D	4.6
Mass ratio m^*	35
Natural frequency [Hz]	1.95
Structural damping ratio $\xi = r/r_c$	$6.5 \cdot 10^{-3} \div 1.4 \cdot 10^{-2}$
Scruton Number	$1.4 \div 2.47$
Aerodynamic characteristics	
Strouhal Number	0.17
Strouhal Velocity [m/s]	8.3

Table 1: Test model mechanical and aerodynamic characteristics

3 TEST RESULTS

3.1 Fixed cylinder

Before the investigations on VIV a preliminary study of the fixed model was achieved in order to define the different Reynolds flow regimes encountered by the cylinder, as described in detail in [3]. Moreover the paper discuss on possible blockage and wall-proximity effects related to the large model dimensions. Figure 2 shows the drag coefficient as a function of the Reynolds Number: for smooth surface condition the drag is about 1 for $Re = 10^5$ and than drops to 0.3. The drag crisis highlights that the cylinder is in the critical Re. At $Re = 140k$, *precritical* regime, the vortex shedding is still visible in the wake of the body (Figure 3(a)) while at higher Reynolds Number the regular vortex shedding disappears and the wake shows a

broad-band spectrum (Figure 3(b)).
In order to increase the effective Reynolds Number [1] the model surface roughness is increased adding a nylon-net (see Figure 1(b)). As well known, surface roughness addiction shifts the drag crisis to lower Reynolds Numbers, permitting to reach high effective *Re* without increasing wind velocity. In rough surface conditions the drag coefficient increases with respect to the minimum reached in the critical regime and it is constant for all the velocity range investigated (Figure 2) and the vortex shedding reappears in the wake (Figure 3(c)). This solution has permitted to extend the investigations on VIV to *postcritical* flow conditions.

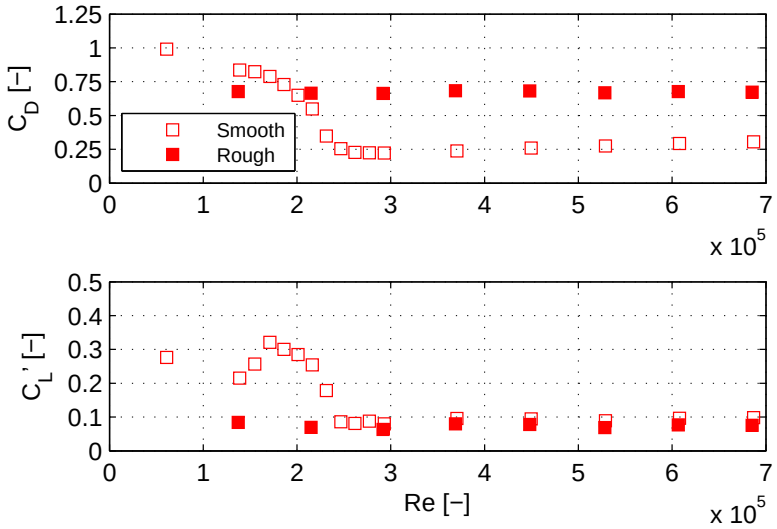

Figure 2: Mean Drag and Lift standard deviation coefficients as a function of Reynolds Number for smooth and rough surface cylinder

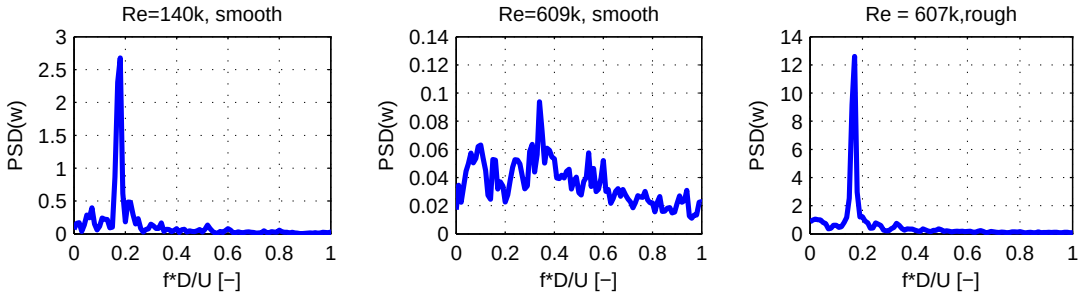

(a) (b) (c)

Figure 3: Wake PSD for different Reynolds Number and surface conditions

3.2 Oscillating cylinder

Two different kind of tests were performed to investigate the vortex induced vibrations: progressive regimes and build-up. The results showed in this section refers to the tests in postcritical flow condition, i.e. with added surface roughness, where relevant vortex induced oscillations where recorded. During progressive regime tests, steady state model response has been studied for different incoming flow velocity: each regime condition was reached starting from the previous one increasing or decreasing the wind speed. Figure 4 shows the main results of these

tests: in Figure 4(a) there is the normalized oscillation amplitude obtained increasing (Up) and decreasing (Down) the incoming wind speed. The maximum displacement $z/D = 0.22$ was reached for velocity ratios close to 1 and it was controlled (*limited*) by an high value of the Scruton Number ($Sc \approx 2$). It was not possible to reach larger amplitudes to avoid large stresses on the constrain structure of the setup. Figure 4(b) and Figure 4(d) describe the characteristics of the fluctuating lift force (the harmonic component at the oscillation frequency) in terms of magnitude and relative phase with respect to the displacement. It is possible to note two different regions: the first one, for $V/V_{St} < 1$, where there are high values of the lift force up to 1.5 and small phase values, close to zero. In the second one, for $V/V_{St} > 1$ the lift force reduces its magnitude but the phase, close to $90\,deg$, is very effective in introducing power into the mechanical system. These two regions are the same as noticed in literature by Khalak and Williamson for the response branches respectively *initial* and *lower* [8]. Figure 4(c) shows the ratio between the actual oscillating frequency and the body natural oscillation frequency in air: a jump phenomenon happens while switching between the two branches and it is related to added mass effects [8]. Generally this jump is well defined for test in water but in this case it is visible also in air due to the low value of the *mass-ratio* of the model. Comparing the data achieved by increasing and decreasing flow velocities an hysteretic behavior is identified and the maximum amplitude, that happens for initial branch conditions, is achieved only for increasing progressive regimes. Also this phenomenon is described in [8] for low Reynolds Number flows.

The simultaneous measurement of the aerodynamic force in three different rings permits the

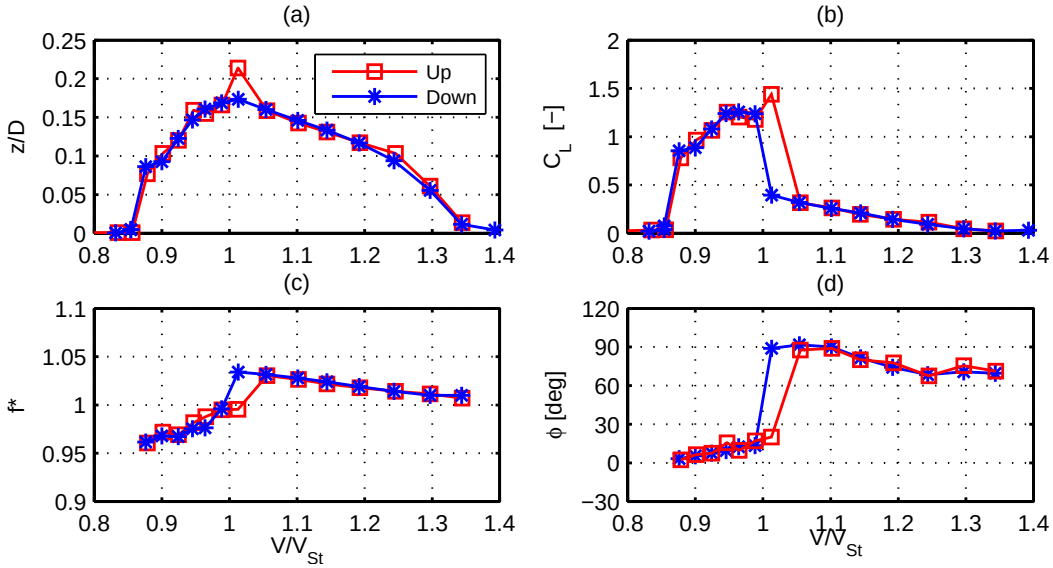

Figure 4: Progressive regime test (rough surface cylinder): non-dimensional amplitude as a function of the normalized velocity V/V_{St} (a), lift force magnitude and phase (b and d), frequency ratio (c). The data are obtained by increasing the wind velocity "Up" and decreasing "Down"

evaluation of the spatial correlation of the force having the cylinder oscillating. Figure 5 shows the cross-correlation of the lift force coefficient: it is clear that the spatial correlation is related to the branch response and it is higher in initial branch conditions respect to the lower branch, even if the cylinder is oscillating at the same amplitude. Moreover in lower branch regime the correlation level seems to be more related to the amplitude than in initial branch.

Build-up tests are very helpful because they permit to define the characteristics of the aerody-

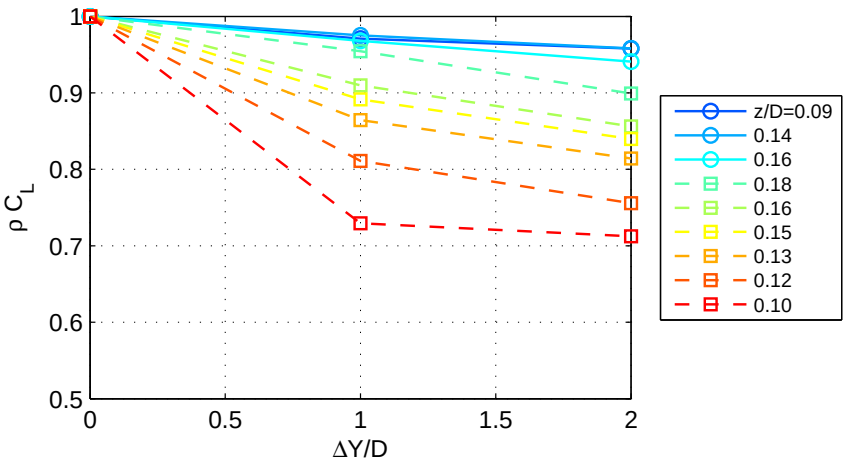

Figure 5: Lift force cross-correlation as a function of the spacing between the rings, for different non-dimensional oscillation amplitudes and velocity-ratios. ◯ Initial Branch, □ Lower Branch

namic forces for all the combinations of z/D and V/V_{St} where the cylinder experiences free motion. An example of build-up test is visible in Figure 6 that shows the lift force, the oscillation amplitude and the relative phase during a build-up transient as a function of the time. The test wind speed, velocity ratio $V/V_{St} = 0.98$, corresponds to initial branch in progressive regime tests. It is possible to see the variation of the aerodynamic force during the transient, in particular the lift force and the oscillation amplitude grow almost simultaneously and the phase shifts from values of about $90\,deg$ to values close to $0\,deg$.

Build-up tests for five different velocity-ratios are summarized in Figures 7 and 8 that show the

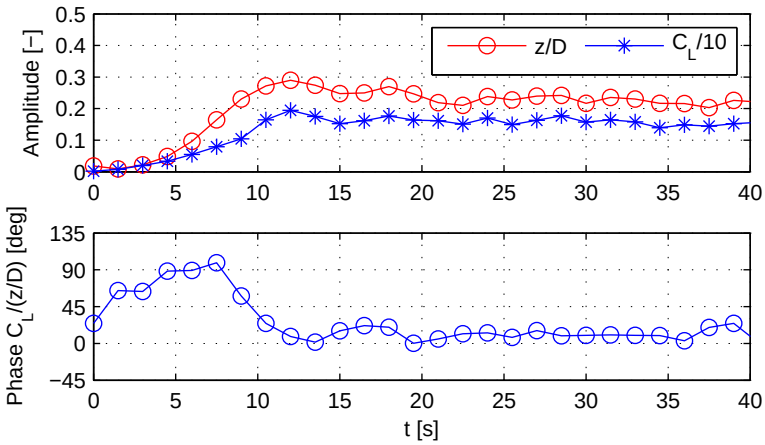

Figure 6: Build-up test results: non-dimensional amplitude and lift magnitude - divided by 10 - (a) and phase between lift force and displacement (b). Data at $V/V_{St} = 0.98$

lift force magnitude and phase as a function of the non-dimensional oscillation amplitude. The first two cases (Figure 7) refers to velocity-ratios less than 1 and they present a transition in the phase and a growing lift coefficient while the vibration amplitudes are becoming larger. The threshold value of nondimensional vibration amplitude when the jump occurs, shifts to higher values increasing the wind velocity. This fact was also noted by the authors in subcritical Reynolds Number tests [14]. The second group of data, $V/V_{St} > 1$, (Figure 8) is characterized by an almost constant value of both the lift force and the phase for all the transient phenomena.

The high value of the phase close to $90\,deg$ is typical of lower branch in progressive regime tests.

The test set-up allows the simultaneous measurement of the aerodynamic force and displace-

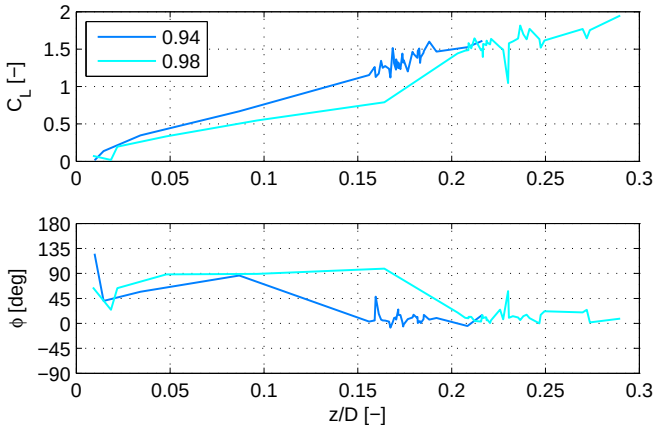

Figure 7: Lift coefficient magnitude and phase as function of the nondimensional amplitude z/D, data for different $V/V_{St} < 1$

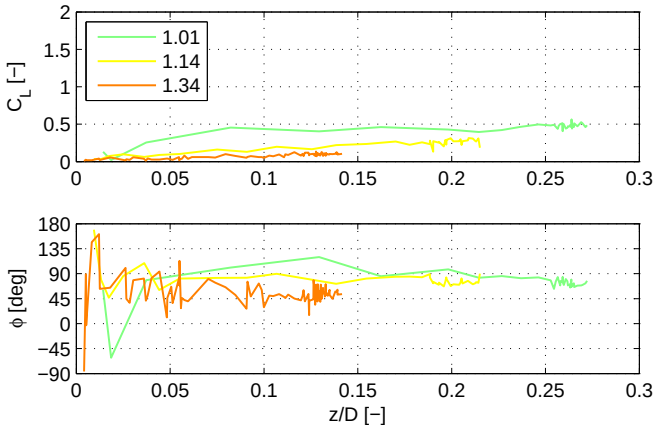

Figure 8: Lift coefficient magnitude and phase as function of the nondimensional amplitude z/D, data for different $V/V_{St} > 1$

ment of the body, giving the possibility to define the power input by the flow into the mechanical system. Figure 9 shows a power input analysis for two different build-up respectively at $V/V_{St} < 1$ and $V/V_{St} > 1$: each point in the graph is evaluated averaging the instantaneous power input over a finite number of cycles. In the first case (Figure 9(a)), after a fast build-up transient, in regime condition the power input is not constant and this is reflected in a slightly variation of the oscillation amplitude during the time history. On the contrary, the second case (Figure 9(b)) is characterized by a lower value of the maximum power input, but a very stable regime condition. As a summary graph Figure 10 reports the envelope curve of the maximum power input compared with previous data in subcritical Reynolds Number flow regime [6, 15]: a generally good agreement among all the data is visible.

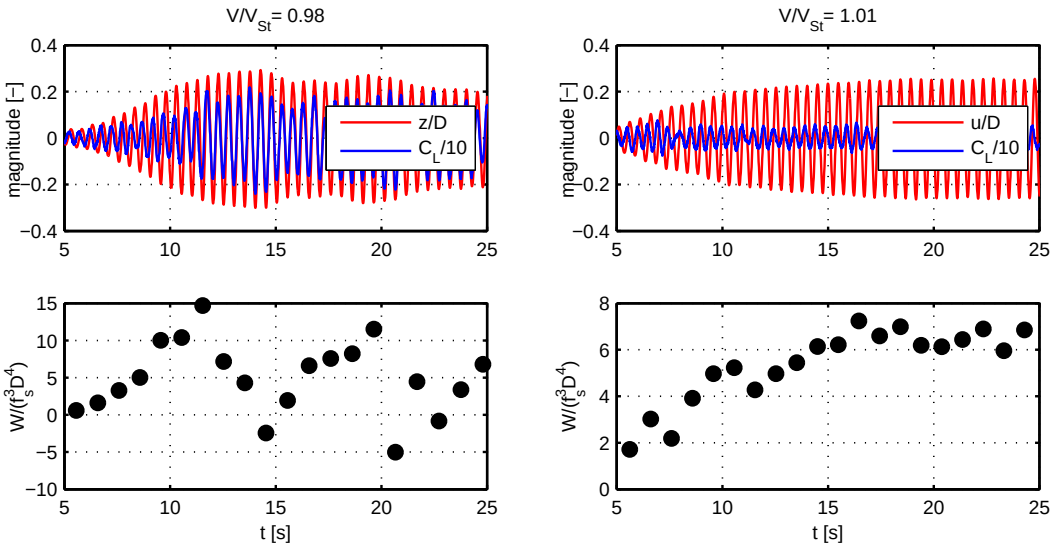

(a) (b)

Figure 9: Build up tests. Lift and displacement time histories and power input averaged over a finite number of cycles: (a) Initial Branch regime conditions ($V/V_{St} < 1$), (b) Lower Branch regime conditions ($V/V_{St} > 1$)

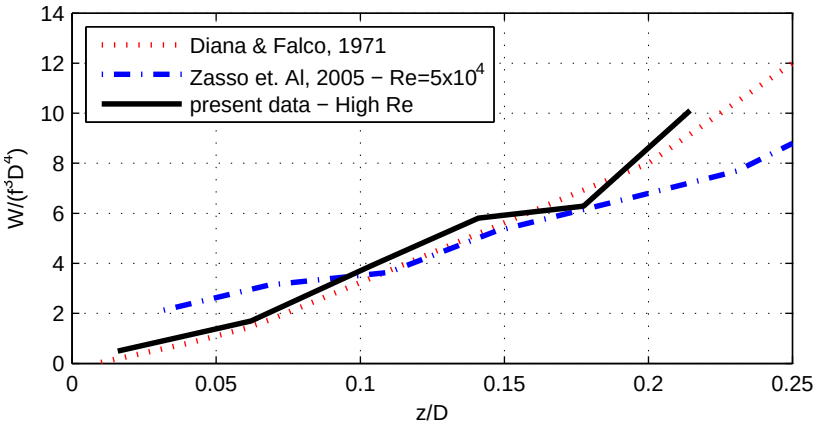

Figure 10: Power introduced by the flow on the oscillating cylinder: comparison of the present experimental data at postcritical Reynolds Numbers with previous ones in subcritical flow regime

4 CONCLUSIONS

The experimental research by wind tunnel tests on a large diameter cylinder allowed the authors to investigate vortex induced vibrations at high Reynolds Number. In particular increasing the surface roughness it has been possible to simulate postcritical flow conditions. In this situation the well correlated vortex shedding reappears when testing on fixed cylinder and the lock-in is found in free oscillation tests. The phenomenon is characterized by progressive regime tests and build-up. The results show the same response branches that are deeply described in literature for low Reynolds Number flows, highlighting that vortex induced phenomena are very similar in the different Reynolds conditions: in detail, basing on the characteristics of the lift force in terms of magnitude and phase a initial branch regime is identified for $V/V_{St} < 1$ and a lower branch for $V/V_{St} > 1$. Unfortunately no upper branch was identified due to the constrains of the test set up that didn't allow oscillations higher that $z/D = 0.3$. Moreover the specific

power input curve shows good agreement among the different Re. This latter fact is very important because numerical models used at low Reynolds could be adopted also in postcritical flow conditions.

5 ACKNOWLEDGEMENTS

The authors wish to acknowledge Dott. Matteo Boiocchi and Dott. Simone Morganti for their help in the research.

REFERENCES

[1] Esdu 80025. Mean forces, pressures and flow field velocities for circular cylindrical structures: single cylinder with two-dimensional flow. 1986.

[2] P. W. Bearman. Vortex shedding from oscillating bluff bodies. *Annual Review of Fluid Mechanics*, 16:195–222, 1984.

[3] M. Belloli, S. Giappino, S. Muggiasca, and A. Zasso. Vortex shedding on circular cylinder at critical and postcritical Reynolds Number. In *Proceedings of the Seventh International Symposium on Cable Dynamics*, 10-13 December 2007.

[4] D. Brika and A. Laneville. Vortex-induced vibrations of a long flexible circular cylinder. *Journal of Fluid Mechanics*, 250, 1993.

[5] Guido Buresti. The effect of surface roughness on the flow regime around circular cylinders. *Journal of Wind Engineering and Industrial Aerodynamics*, 8(1-2):105–114, 1981.

[6] G. Diana and M. Falco. On the forces transmitted to a vibrating cylinder by a blowing fluid. *Meccanica*, 6(1), 1971.

[7] R. Govardhan and C.H.K. Williamson. Modes of vortex formation and frequency response of a freely vibrating cylinder. *Journal of Fluid Mechanics*, 420:85–130, 2000.

[8] A. Khalak and C. H. K. Williamson. Motions, forces and mode transitions in vortex-induced vibrations at low mass-damping. *Journal of Fluids and Structures*, 13(7-8):813–851, 1999.

[9] A. Roshko. Experiments on the flow past a circular cylinder at very high Reynolds Number. *Journal of Fluid Mechanics*, 10(3):345–356, 1961.

[10] T. Sarpkaya. Vortex-induced oscillations. A selective review. *Journal of Applied Mechanics*, 46, 1979.

[11] T. Sarpkaya. A critical review of the intrinsic nature of vortex-induced vibrations. *Journal of Fluids and Structures*, 19(4):389–447, 2004.

[12] C. H. K. Williamson and R. Govardhan. Vortex-induced vibrations. *Annual Review of Fluid Mechanics*, 36:413–455, 2004.

[13] C. H. K. Williamson and A. Roshko. Vortex formation in the wake of an oscillating cylinder. *Journal of Fluids and Structures*, 2:355–381, 1988.

[14] A. Zasso, M. Belloli, S. Giappino, and S. Muggiasca. Pressure field analysis on oscillating circular cylinder. *Journal of Fluids and Structures, in stampa*, 2008.

[15] A. Zasso, A. Manenti, M. Belloli, S. Giappino, and S. Muggiasca. Energy input by the flow on a vibrating smooth circular cylinder in cross flow at Re=5x104. In *Proceedings of the Sixth International Simposium on Cable Dynamics*, September 19-22, 2005 2005.

[16] M. M. Zdravkovich. *Flow around circular cylinders, Vol. 1: Foundamentals*. Oxford University Press, Oxford; New York, 1997.